•.

Letter to the Editor: first results from ISO

ISM parameters in the normal galaxy NGC 5713*

S. 1). Lord[1], S. Malhotra[1], T. Lim[2], G. Helou[1], C. A. Beichman[1], 11. Dinerstein[3], I). J. Hollenbach[4], 1). A. Hunter[5], K. Y. J,o[6], N. Y. Lu[1], R. H. Rubin[4], G. J. Stacey[7], Ii. A. Thronson Jr.[8], and M. W. Werner[9]

[1] I]'AC, California Institute of Technology, MS 10022, Pasadena, CA 91125
[2] ESA Villafranca Satellite Tracking Station, Apartado 50727 28080 Madrid, Spain
[3] University of Texas, Astronomy Department, RLM 15.308, Texas, Austin, TX 78712
[4] NASA/ Ames Research Center, MS 245-6, Moffett Field, CA 94035
[5] Lowell Observatory, 1400 Mars Hill Rd, Flagstaff, AZ 86001
[6] University of Illinois, Astronomy Department, 1002 W. Green St., Urbana, II, 61801
[7] Cornell University, Astronomy Department, 220 Space Science Building, Ithaca, NY 14853
[8] University of Wyoming, Wyoming Infrared Observatory, Laramie, WY, 82071
[9] Jr-t Propulsion laboratory, MS 233-303, 4800 Oak Grove Rd., Pasadena, CA 91109

Received August 8, 1996; accepted 1996

Abstract. We report 1S() Long Wavelength Spectrometer (LWS) observations of the Sbc(s) pec galaxy NGC 5713. We have obtained strong detections of the fine-structure forbidden transitions [C II] 158 μm, [O I] 63 μm, and [O III] 88 pm) and significant upper limits for [N II] 122 μm, [O III] 5'2 μm, and [N III] 57 μm. We also detect the galaxy's dust continuum emission between 43 and 197 microns. The 80" half-power beam diameter of the LWS instrument corresponds to roughly 11 kpc at the distance of NGC 5713, and should therefore collect the total emission from the galaxy.

The measurements of the continuum and the [C II] and [0 I] line fluxes have been combined Lo derive the temperature and density of the warm atomic gas surrounding molecular clouds and the UV flux incident on the clouds, We find higher densities and lower UV fluxes in NGC 5713 than arc typical for starburst galaxies.

Key words: Galaxies: individual/NGC 5713; galaxies: ISM; infrared: spectroscopy, galaxies

Send offprint requests to: S. Lord

*Based on observations with 1S0, an ESA project with instruments funded by ESA Member States (especially the PI countries: France Germany, the Nettler lands and the United Kingdom) and with the participation of ISAS and NASA

1. Introduction

We report the first spectroscopic observations from the infrared Space Observatory (ISO; Kessler et al. 1996) under the US Guaranteed Time project on the interstellar medium of star-forming galaxies (Helou et al. 1996). We used the 1S0 LWS (Clegg et al. 1996) to measure the total flux in six transitions from NGC 5713, one of approximately sixty galaxies in Lhc project.

NGC 5713 is an Sbc(s) pcc galaxy at a redshift of 1883 km s^{-1}, implying a distance of 24 Mpc for $H_0 = 75$ krn S--1 Mpc^{-1} assumed hereafter. It has multiple spiral arms which originate near the center and maintain high surface brightness for about 1/2 revolution out to 30". Beyond this radius, there is only a single smooth and continuous arm of low surface brightness, earning this system its "pee" morphological label. IRAS observations indicate the FWHM of the 60 μm emission Lo be less than 60" while the optical disk extends to 120" in diameter. Active star formation is indicated by H II regions situated on the inner arm fragments.

With its intermediate values of FIR luminosity $L_{FIR} = 2 \times 10^{10} L_{\odot}$, and infrared-to blue luminosity ratio of about 2, this galaxy is relatively active in star formation, though not au extreme "star-burst" system. Part of a small cluster of predominantly]atc-type spirals, NGC 5713 may be interacting with its neighbors, the nearest of which, NGC 5719, lies at a projected distance of 60 kpc. However, NGC 5713 possesses a fairly low FIR to molecular emission ratio, $L_{FIR}/L_{CO} < 25$, as compared to other in-

Fig. 1. NGC 5713 LWS atomic fine structure lines

teracting intermediate luminosity systems, for which the ratio is typically 75. The FIR/CO ratio for NGC 5713 is more characteristic of an isolated spiral (Tinney CL al. 1990).

2. Observations and Analysis

NGC 5713 was observed during 1S0's Performance Verification period using the LWS grating line-mode AOT, LWS02, with the 80" FWHM beam of the LWS encompassing the entire infrared bright central disk. Each of six lines was observed for a time between 6 and 100 seconds per spectral element. All lines were unresolved by the instrument (see Figure 1), with $\lambda/\Delta\lambda$ -200, and the detected lines appeared at the expected wavelengths, adjusted for the galaxy's redshift. Flux calibration included the application of in-orbit detector responsivity values modeled as a function of time. Post-pipeline processing was accomplished with the 1S0 Spectroscopy Analysis Package, ISAP, specifically using the Rutherford Appleton Laboratory's Graphic User Interface (RAL GUI) designed for the purpose. About 90% of the data were determined to be free of detector gain drifts due to cosmic ray hits, and were retained in the reduction. Mean and median averaging of the data taken at a given wavelength yielded virtually identical results.. Line fluxes were determined by direct integration of the profiles. Upper limits for the three non-detections arc the multiplicative product. of 3 times the rms of the scans and a wavelength interval equal 10 the detector resolution element.

The 1S0 LWS continuum flux densities deviate substantially from the spectrum expected for NGC 5713 from the IRAS data assuming a superposition of blackbody components (Table 1). They arc 1.5 to 2 times too high at short wavelengths. This disagreement may be due to mis-calibration of the 1S0 data, either because of overestimated detector responsivities or under-rxtimated dark currents. In the first case the line fluxes would suffer the same overestimation as the continuum, whereas in the second they would be more accurate than the continuum. In the absence of conclusive evidence as 10 its cause, this disagreement was used to bound the uncertainty on the LWS fluxes by considering three possibilities: (1) all LWS data arc correct as reduced; (2) both continuum and line fluxes from LWS have to be scaled so the continuum agrees with the I1tAS-based estimates; and (3) LWS line fluxes arc correct, but the continuum is given by the IRAS estimates. The three sets of values were carried through the subsequent analysis, and yielded the ranges plotted in Fig. 2, 3 and 4.

The statistical errors for the line fluxes of the detected lines were relatively small: less than 5% for the three detections. However, the uncertainty discussed in the preceding paragraph dominates, and amounts to 30% for the CII line and a factor of 2 for the OI line.

Table 1. NGC 5713 Spectroscopy Results from LWS Observations

Species	λ_0 (μm)	Line Flux (10^{-19} W/cm^2)	Continuum[a] (LWS; Jy)	Continuum[a] (IRAS; Jy)
[OIII]	51.8	<5.6	3G	14
[NIII]	57.3	<1.0	37	17
[OI]	63.2	3.1	43	20
[OIII]	88.4	2.4	54	32
[NiI]	121.9	<1.5	44	43
[CII]	157.7	8.3	49	39

[a]The observed 1S0 continuum flux density and the predicted continuum flux density bawd on IRAS measurements.

3. Physical Conditions

The detected line fluxes (Table 1) are within the range observed by the Kuiper Airborne Observatory in active star-forming galaxies (Figures 2- 4): The [O I] and [C II] fluxes in NGC 5713 arc several parts per thousand of the FIR continuum, and the line-to-continuum ratios for the three detected lines arc within a factor of three of the values observed in M82 (Lord et al. 1996a). As detailed below however, a closer look rc.veals significant differences between NGC 5713 and previously studied star-burst galaxies. In comparison to the KAO facility background-limited instrument sensitivities (e.g. Erickson et al. 1995), these observations with the ISO LWS have reached about 5- 10 times lower flux levels, particularly between 51 and 88 μm.

Fig. 2. ISO/LWS NGC 5713 results compared with KAO sample of IR-bright galaxies (Lord et al. 1996b) showing [01] 63 μm vs. FIR cord, nuum. The three data points shown for NGC 5713 correspond to the three cases discussed in §2, ○ for case (1); ⊗ for case (2); and ◐ for case (3).

Wc interpret the [O I] and [C II] lines in the context of photodissociation region models (Wolfire, Tielens, & Hollenbach 1990, hereafter W']'] 1, and Tielens & Hollenbach

Fig. 3. [CII] 158 μm vs. FIR continuum. See Fig. 2 caption.

Fig. 4. [01 1] 88 μm vs. FIR continuum. See also Fig. 2 caption.

1985). In I GC 5713, the ([C II]+[O I])/FIR ratio is high, between 0.6 and 0.7%. This indicates a relatively high ratio of the atomic gas density, n, to UV illumination, Go, where Go is the UV radiation field strength measured in units of the local interstellar radiation field of the Milky Way. For this FIR line to continuum ratio, $n/G_0 = 50$. The FIR line to continuum ratio measured in the starburst galaxies shown in Figure 2 range from 0.2 to 0.7%, with a median value of 0.5%, and a corresponding ratio $n/G_0 = 15$. The [C II]/[O I] ratio in NGC 5713 is between 3 and 5, which is distinctly higher than in starburst systems, where this ratio is typically close to 1.0 (Lord et al. 1996b). For NGC 5713, the atomic line ratio and the line to continuum ratio arc consistent with regions of high atomic gas density, log(n) ~ 4.2 and low UV illumination, $\log(G_0) \sim 2.8$.

In the domain of low Go, (log(Go) < 3.0), atomic gas temperatures can be low, T< 200 K, and the upper [O I] energy state ($\Delta E/K \sim 280$ K) depopulates more rapidly than the [C II] upper energy state ($\Delta E/K \sim 901\{\}$), yielding high CII/OI ratios. In regions with high atomic gas heating from photoejected electrons is efficient because high densities grains remain less positively charged.

It is also possible that within the NGC 5713 disk, a diffuse gas component contributes CII flux and that this is in part responsible for the high CII/OI ratio seen. The OI transition has a high critical density, $n_{cr} \sim 5 \times 10^5$ cm^{-3}, above which collisional de-excitation becomes important, and so negligible contribution is expected from diffuse gas regions. Even though the CII/OI ratio may be affected, most likely the CII/FIR ratio in diffuse regions is similar to that in PDRs and so the (CII+OI)/FIR will be affected less. Our ISO program includes a series of [C II] observations of diffuse gas regions in nearby galaxies which will test this hypothesis.

We have modeled the ionized component of the ISM in this galaxy using the H II region models of Rubin et al. (1991). By comparing emission lines of the same element, we can determine the electron density, n_e, in these regions and the effective temperature, T_{eff}, of the ionizing stars, and do so independently of any elemental abundance assumptions.

The upper limit on the [O III] 88 μm/[O III] 52 μm flux ratio of 0.43 constrains the typical H II region electron density to $n_e < 10^3$ cm^{-3}, which is within the expected range for normal H II regions.

The [N III]/[N II] ratio probes the maximum effective stellar temperature in the H II regions. Taking the N III 57 μm result as a tentative 3.4 σ detection, then the upper limit [N III]/[N II] < 0.67 gives T_{eff} < 36,000 K (Rubin et al. 1991), corresponding to a 20 $M_\odot$ upper limit to the stellar mass distribution. We note this result is consistent with the findings of Doherty et al. (1995) for NGC 5713, who use their measured value of the HeI (2.058 μm)/Brγ ratio of 0.32 for this galaxy to constrain the typical T_{eff}. Depending on the primordial helium abundance and HII region electron temperature assumed, they find a T_{eff} range between 35,000 and 37,500 K for NGC 5713.

We contrast our results with those found using the ISO LWS for the collisional galaxy system NGC 4038/39 (Fischer et al. 1996). Fischer et al. find a UV field with $log(G_0)$ as high as 3.5, which is an order of magnitude higher than what we find in NGC 5713. This higher value of G_0 is typical for moderate star-bursts and is consistent with other tracers of strong star formation activity seen in NGC 4038/39.

4. Conclusions

1. The detected lines have flux values (within uncertainties) that are consistent with their origin in photodissociation regions ([C II] 158 μm, [O I] 63 μm) and ionized regions ([O III] 88 μm). The LWS detections reach 5-10 times fainter fluxes than achieved on the KAO.
2. The [C II] emission is unexpectedly strong: about 0.6% of the FIR continuum.
3. Photodissociation regions in NGC 5713 tend toward low UV illumination of the atomic gas, $\log(G_0) \sim 2.8$, and high atomic gas density, $\log(n) \sim 4.2$. For comparison, typical starburst galaxies have $\log(G_0) \sim 3.5$ and the inner 5 pc of the Galactic Center exhibits $\log(G_0) = 4.9$ (WTH).
4. The [O III] 88 μm flux and the [O III] 52 μm upper limit indicate an H II region electron density, $n_e < 10^3$ cm^{-3}, indicative of normal H II regions. Using the upper limit of the ionized nitrogen line ratio, and taking the 57 μm as a possible 3.4 σ detection, [N II]/[N III] < 1.2 gives an upper limit to the maximum effective stellar temperature of stars in these regions, T_{eff}, with T_{eff} <36,000 K.

Acknowledgements. This work was supported in part by ISO data analysis funding from the US National Aeronautics and Space Administration, and carried out at the Infrared Processing and Analysis Center and the Jet Propulsion Laboratory of the California Institute of Technology. We thank the LWS Instrument Dedicated Team for including this observation in their Performance Verification phase, and their continuing assistance in the data analysis.

References

Doherty, R. M., Puxley, P. J., Lumsden, S. L., Doyon, R., 1995, MNRAS, 277, 577
Erickson, E. F., Colgan, S. W. J., Simpson, J. P., Rubin, R. H., 1995, ASP Conf. Series 73, ed. M. R. Haas, J. A. Davidson, & E. F. Erickson, p. 523
Fischer, J. et al. 1996, this volume,
Helou, G. et al. 1996, this volume.
Kessler et al. 1996, this volume.
Lord, S. D., Hollenbach, D. J., Haas, M. R., Rubin, R. H., Colgan, S. W. J., Erickson, E. F., 1996a, ApJ, 465, 000
Lord, S. D., et. al, 1996b, in preparation
Rubin, R. H., Simpson, J. P., Haas, M. R., Erickson, E. F. 1991, ApJ, 374, 564
Tielens A. G. G. M., Hollenbach D., 1985, ApJ, 291, 722
Tinney, C. G., Scoville, N. Z., Sanders, D. B., Soifer, B. T., 1990, ApJ, 362, 473
Wolfire M., Tielens A. G. G. M., Hollenbach D. J., 1990 ApJ, 358, 116 (WTH)

This article was processed by the author using Springer-Verlag LaTeX A&A style file L-AA version 3.

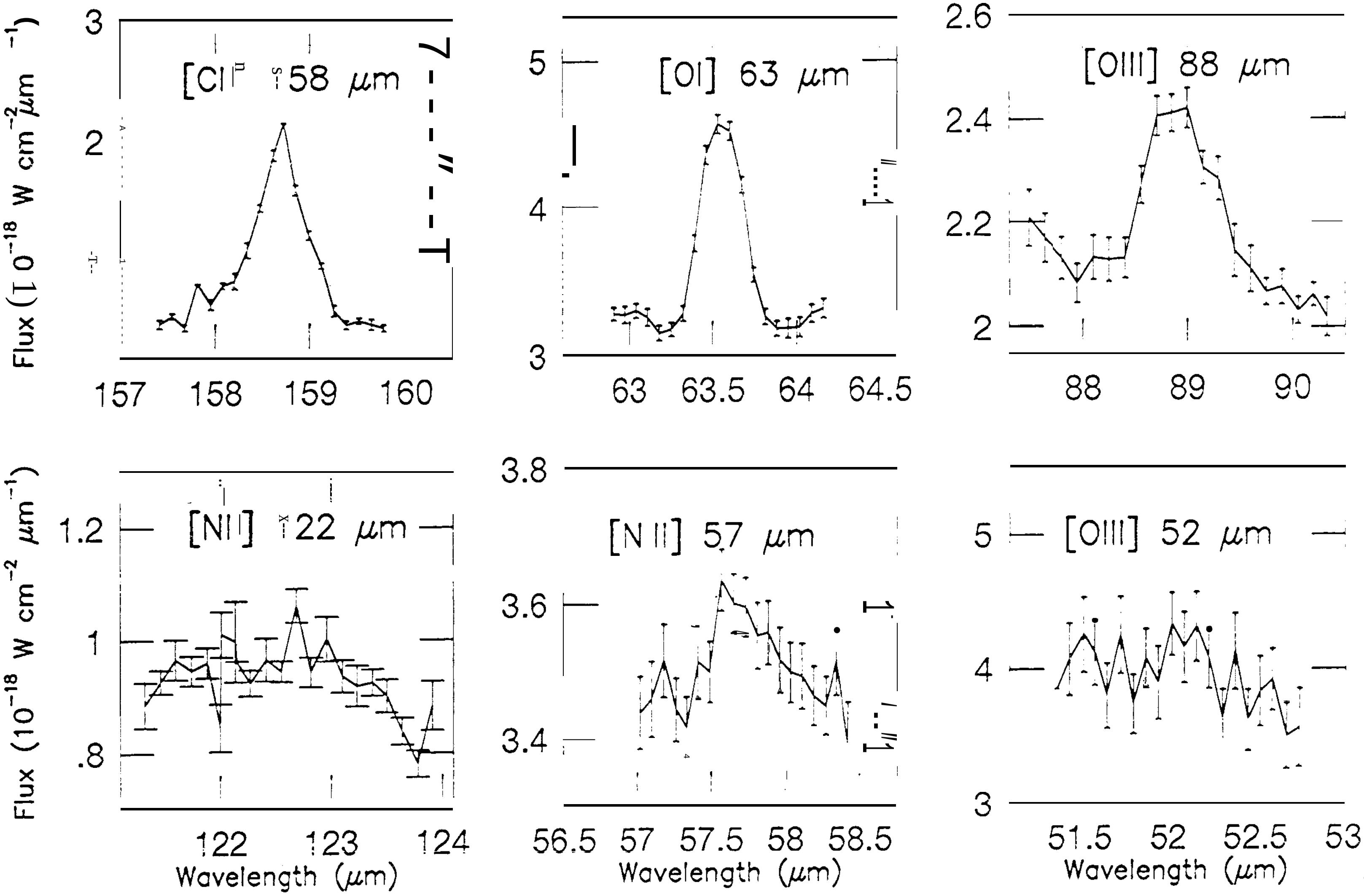

[CII] 158 μm
[OI] 63 μm
[OIII] 88 μm
[NII] 122 μm
[N II] 57 μm
[OIII] 52 μm
Flux (10^{-18} W cm^{-2} μm^{-1})
Wavelength (μm)

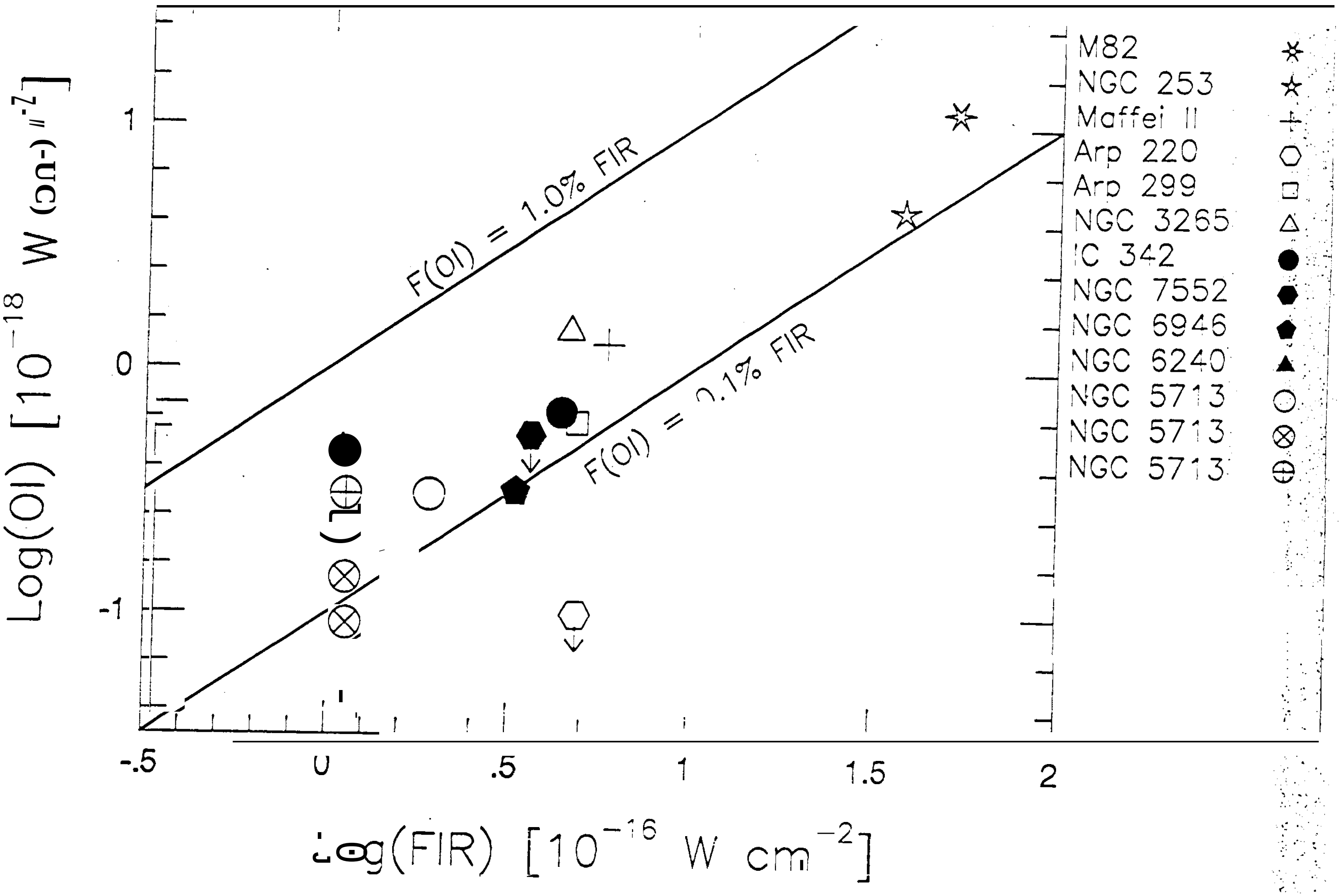

M82
NGC 253
Maffei II
Arp 220
Arp 299
NGC 3265
IC 342
NGC 7552
NGC 6946
NGC 6240
NGC 5713
NGC 5713
NGC 5713
F(OI) = 1.0% FIR
F(OI) = 0.1% FIR
Log(OI) [10^-18 W cm^-2]
Log(FIR) [10^-16 W cm^-2]
-.5
0
.5
1
1.5
2
1
0
-1

2 (revised)

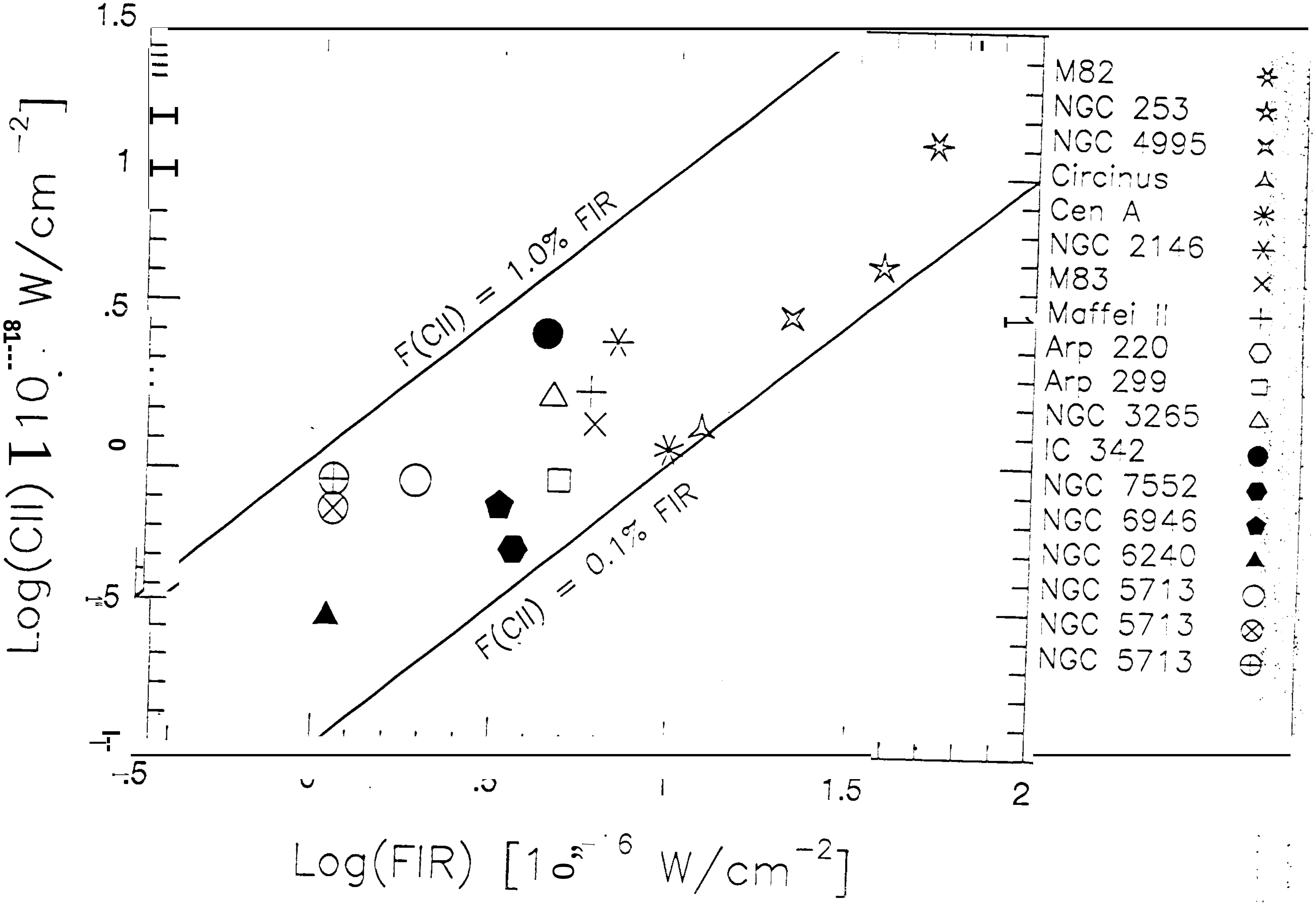

M82
NGC 253
NGC 4995
Circinus
Cen A
NGC 2146
M83
Maffei II
Arp 220
Arp 299
NGC 3265
IC 342
NGC 7552
NGC 6946
NGC 6240
NGC 5713
NGC 5713
NGC 5713
F(CII) = 1.0% FIR
F(CII) = 0.1% FIR
1.5
1
.5
0
-.5
-1
1.5
2
Log(CII) [10^-18 W/cm^-2]
Log(FIR) [10^-6 W/cm^-2]

3 (revised)

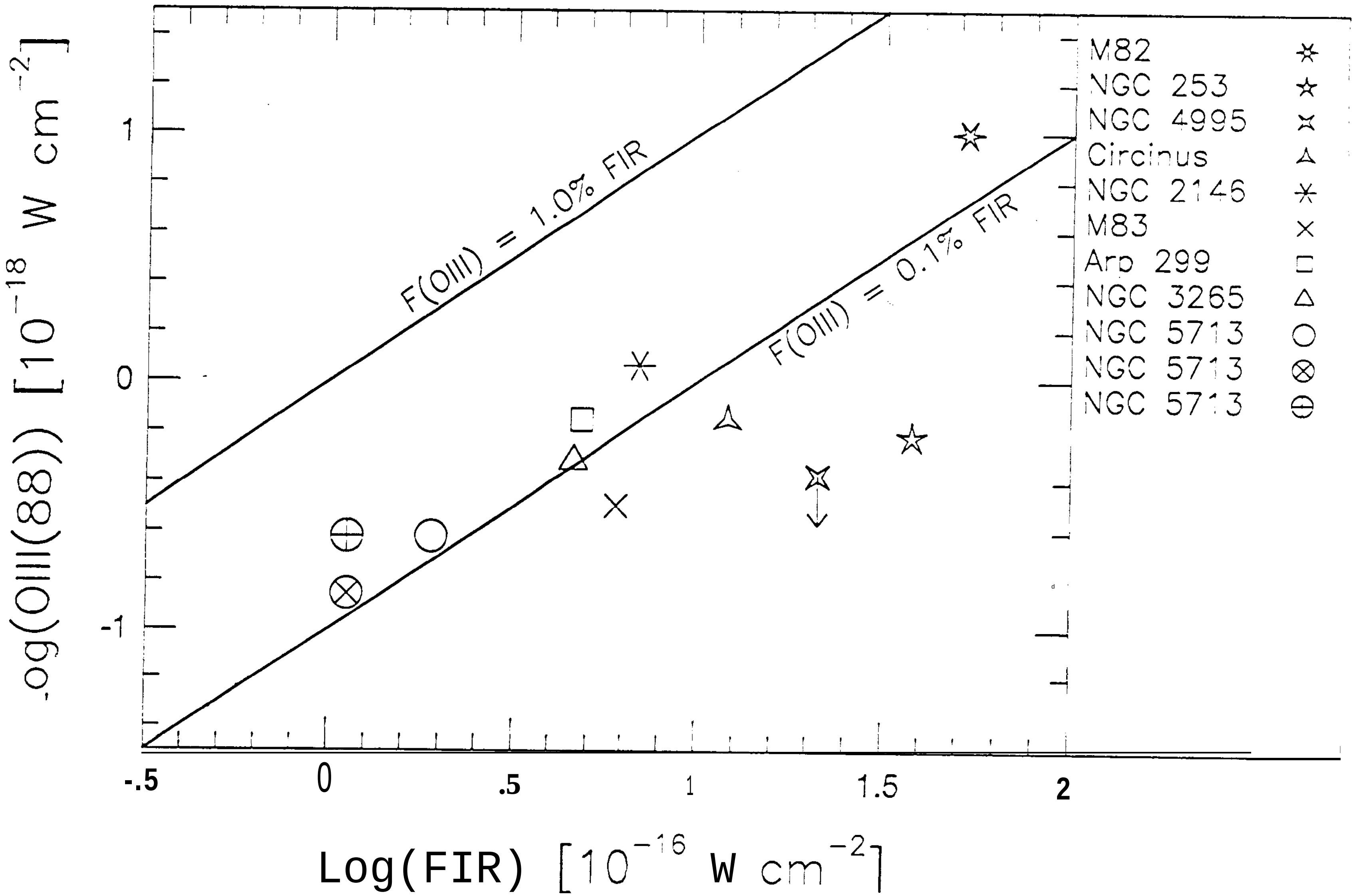
F(OIII) = 1.0% FIR
F(OIII) = 0.1% FIR
M82
NGC 253
NGC 4995
Circinus
NGC 2146
M83
Arp 299
NGC 3265
NGC 5713
NGC 5713
NGC 5713
1
0
-1
-.5
0
.5
1
1.5
2
Log(FIR) [10^-16 W cm^-2]
Log(OIII(88)) [10^-18 W cm^-2]

4 (revised)